NASA/TM- -97- 208111

Accuracy of Aerodynamic Model Parameters Estimated from Flight Test Data

Eugene A. Morelli*

Lockheed Martin Engineering and Sciences Company, Hampton, Virginia 23681-0001

and

Vladislav Klein†

George Washington University and NASA Langley Research Center, Hampton, Virginia 23681-0001

An important part of building mathematical models based on measured data is calculating the accuracy associated with statistical estimates of the model parameters. Indeed, without some idea of this accuracy, the parameter estimates themselves have limited value. An expression is developed for computing quantitatively correct parameter accuracy measures for maximum likelihood parameter estimates when the output residuals are colored. This result is important because experience in analyzing flight test data reveals that the output residuals from maximum likelihood estimation are almost always colored. The calculations involved can be appended to conventional maximum likelihood estimation algorithms. Monte Carlo simulation runs were used to show that parameter accuracy measures from the new technique accurately reflect the quality of the parameter estimates from maximum likelihood estimation without the need for correction factors or frequency domain analysis of the output residuals. The technique was applied to flight test data from repeated maneuvers flown on the F-18 High Alpha Research Vehicle. As in the simulated cases, parameter accuracy measures from the new technique were in agreement with the scatter in the parameter estimates from repeated maneuvers, whereas conventional parameter accuracy measures were optimistic.

Nomenclature

a_z	= vertical acceleration, g
C_L	= lift coefficient
C_M	= pitching moment coefficient
C_Z	= vertical force coefficient
$\bar{c}$	= mean aerodynamic chord, ft
D	= dispersion matrix
d_{jj}	= jth diagonal element of D
$E\{\cdot\}$	= expected value
$e(i)$	= ith equation error residual
g	= gravitational acceleration, 32.174 ft/s²
I_y	= pitch axis moment of inertia, slug-ft²
J	= cost function
M	= information matrix
m	= mass, slug
N	= total number of sample times
n_o	= number of outputs
n_p	= number of parameters
q	= body axis pitch rate, rad/s
$\bar{q}$	= dynamic pressure, lbf/ft²
R	= discrete noise covariance matrix
$\mathfrak{R}_{vv}$	= autocorrelation matrix of vector v
S	= wing area, ft²
$S(i)$	= output sensitivity matrix at time $(i - 1)\Delta t$
s	= sample standard error
t	= time, s
$u(t)$	= control vector
V	= airspeed, ft/s
$v(i)$	= output residual vector at time $(i - 1)\Delta t$
$x(t)$	= state vector
$y(i)$	= $n_o \times 1$ output vector at time $(i - 1)\Delta t$
$y(t)$	= $n_o \times 1$ output vector
$z(i)$	= ith measured scalar
$z(i)$	= measured $n_o \times 1$ output vector at time $(i - 1)\Delta t$
α	= angle of attack, rad
Δt	= sample time, s
δ_{ij}	= Kronecker delta
δ_s	= stabilator deflection, rad
Θ	= pitch angle, rad
θ	= element of the parameter vector θ
θ	= $n_p \times 1$ parameter vector
σ	= Cramér–Rao bound for the standard error of $\hat{\theta}$
$v(i)$	= measurement noise vector at time $(i - 1)\Delta t$
∇_θ	= gradient with respect to θ
Φ	= roll angle, rad
$\mathbf{0}$	= zero vector

Subscripts

c	= corrected
m	= measured
o	= initial or bias
w	= wind axes

Superscripts

T	= transpose
-1	= matrix inverse
$\hat{}$	= estimate
$\bar{}$	= mean value
$\cdot$	= time derivative

Introduction

AIRCRAFT dynamic models include parameters that quantify the dependence of aerodynamic forces and moments on state and control variables. The values of these parameters are often estimated from flight test data. A good quantitative assessment of the accuracy of these parameter estimates is important for a variety of reasons related to experiment design, modeling, simulation, and flight control.

Maximum likelihood[1,2] is commonly used to estimate aerodynamic parameters from flight test data. Assuming the model

Accuracy of Aerodynamic Model Parameters
Estimated from Flight Test Data

E. A. Morelli and V. Klein

structure is correct, maximum likelihood parameter estimates approach the true parameter values, and the parameter variances approach their theoretical minimum values (the Cramér–Rao lower bounds), as the number of measured data points increases. Generally, a flight test data record length at least two to three times the period of the slowest dynamic mode to be modeled is sufficient for the parameter variances to closely approach the Cramér–Rao bounds.[3] In such cases, the Cramér–Rao bound can be used as a good approximation to the variance of maximum likelihood parameter estimates. References 3–5 compare and contrast the Cramér–Rao bound with other methods for assessing the accuracy of parameter estimates. Theoretical properties of maximum likelihood estimators and related arguments discussed in Ref. 3 indicate that the Cramér–Rao bound is the best accuracy measure for maximum likelihood parameter estimates.

The research described here focuses on the output error formulation of maximum likelihood parameter estimation. This formulation includes measurement noise, but no process noise.[1,2] A modified Newton–Raphson optimization procedure[6] was used to determine the maximum likelihood parameter estimates. With this approach, the Cramér–Rao bounds are computed as part of the estimation procedure. It is well known, however, that the Cramér–Rao bounds computed in this way are usually optimistic (too small) compared to the scatter in the parameter estimates from repeated flight test maneuvers.[3,7] This prompted the work of Maine and Iliff[2,3] (also Refs. 8 and 9) and Balakrishnan and Maine,[10] who traced the discrepancy to the fact that the output residuals are colored for real flight test data analysis because some deterministic modeling error is always present. Output error techniques lump the deterministic modeling error together with the broadband random part of a measured signal and call this the measurement noise. This means the measurement noise is model dependent and colored, because the deterministic modeling error usually lies in the same frequency band as the aircraft rigid body dynamics and accounts for a large part of the total noise power. References 2, 3, and 8–10 describe how this kind of colored measurement noise is responsible for the discrepancy between the conventional calculation of the Cramér–Rao bounds and the observed scatter in flight-determined parameter estimates from repeated maneuvers.

The theory underlying the output error formulation of maximum likelihood estimation assumes that the measurement noise is white Gaussian and band limited by the Nyquist frequency. The band limit is the result of discrete measurements taken at the sampling frequency, which is twice the Nyquist frequency. This measurement noise is broadband and incoherent. The term incoherent implies amplitude discontinuity and a lack of consistent phase-amplitude relationships, causing the autocorrelation function to be close to the impulse function. This part of the residual would be commonly recognized as having no deterministic component. If the structure of the model were correct, the residuals would be expected to be reasonably close to this type of noise. In real flight test data analysis, however, the residuals contain deterministic components from such sources as approximations to real aircraft aerodynamic dependencies, unmodeled dynamics such as structural modes, and linearization of the equations of motion. The result is colored residuals, which violate the assumption of white measurement noise in conventional maximum likelihood theory, leading to the aforementioned discrepancy.[2,3,8–10]

In Ref. 3, several engineering solutions were proposed to correct for the discrepancy. Each solution was based on the assumption that most of the power in the output residuals for real flight data analysis is concentrated in roughly the same frequency band as the rigid body dynamics and is due to deterministic modeling error. This assumption is stretched when relatively high-frequency structural modes appear in the data or when the broadband random noise has a large enough magnitude to rival the power of the narrow-band noise due to deterministic modeling error. For multiple outputs, the noise power from broadband random noise compared to that from narrow-band deterministic modeling error is different for each output because of differences in the sensor characteristics and the physical quantity being measured. The solutions offered in Ref. 3 depend on knowing something about the bandwidth of the dominant source of power

in the residuals. Obtaining this information requires Fourier transforms of the residuals and analysis in the frequency domain. The spectra of the residuals depend on the model structure, the maneuver, the flight condition, and the instrumentation characteristics. All of these factors can change over the course of a flight test program, requiring changes in the corrections for the Cramér–Rao bounds. In addition, the bandwidths of the deterministic modeling error for the various measured outputs can be different from one another for the same maneuver. The solutions from Ref. 3 require some engineering judgment in the form of determining a correction factor or estimating the bandwidth of the dominant power in the residuals. Both of these approaches require an experienced analyst and limit the accuracy of the results.

In the present work, a technique first put forth in Ref. 11 was used to process the residuals from a conventional maximum likelihood estimation to compute accurate Cramér–Rao lower bounds for colored residuals. The approach accounts for colored residuals using a simple estimate of the residual correlation in the time domain. Existing maximum likelihood estimation routines can be easily upgraded because the technique involves a postprocessing of the output residuals to correct the Cramér–Rao lower bounds from the conventional calculation. The purpose of the present work is to document a few refinements and extensions, to validate the technique using Monte Carlo simulation with colored measurement noise, and to apply the technique to real data from repeated flight test maneuvers.

The next section contains the theoretical analysis. Following this, the technique was applied in a controlled situation using simulated data from a model of the longitudinal dynamics of a fighter aircraft. The true parameter values were known, and the measured outputs were corrupted with colored noise, including both narrow-band modeling error and broadband random noise. Using 200 Monte Carlo simulation runs with various colored noise characteristics, it was demonstrated that the new technique produces Cramér–Rao bounds representative of the observed scatter in the parameter estimates. The conventional Cramér–Rao bounds were found to be optimistic, in agreement with the results of previous research.[2,3,7–10]

The technique was then applied to repeated longitudinal flight test maneuvers at 20-deg angle of attack for the F-18 High Alpha Research Vehicle (HARV). The scatter in the model parameter estimates from this flight test data was consistent with the Cramér–Rao bounds computed using the new technique, whereas the conventional calculation again gave optimistic values for the Cramér–Rao bounds.

Theoretical Development

The aircraft dynamic model can be represented as

$$\dot{x}(t) = f[x(t), u(t), \theta] \tag{1}$$

$$x(0) = x_o \tag{2}$$

$$y(t) = g[x(t), u(t), \theta] \tag{3}$$

$$z(i) = y(i) + v(i) \qquad i = 1, 2, \ldots, N \tag{4}$$

For conventional maximum likelihood, the discrete measurement noise vector $v(i)$ is assumed to be zero mean white Gaussian and band limited at the Nyquist frequency,

$$E\{v(i)\} = 0 \qquad E\{v(i)v^T(j)\} = R\delta_{ij} \tag{5}$$

The maximum likelihood estimate of the parameter vector maximizes the conditional probability density function[1,6]

$$\hat{\theta} = \arg\max_{\theta}[p(Z \mid \theta)] \tag{6}$$

where Z is the set of all measurement vectors $z(i)$, for $i = 1, 2, \ldots, N$. When R is known, maximizing the conditional

probability in Eq. (6) is equivalent to minimizing the cost function[1-3,6,11]

$$J(\theta) = \frac{1}{2} \sum_{i=1}^{N} [z(i) - y(i)]^T R^{-1} [z(i) - y(i)] \qquad (7)$$

The cost in Eq. (7) can be minimized using a modified Newton–Raphson technique[6] to determine parameter updates, starting from some initial guess of the parameter vector. The initial guess for the parameter vector can be obtained from equation error methods,[7] but, typically, a much rougher initial guess can be used.

The sensitivity matrix is defined as

$$S(i) \equiv \left. \frac{\partial y(i)}{\partial \theta} \right|_{\theta = \hat{\theta}} \qquad i = 1, 2, \ldots, N \qquad (8)$$

where the jth column of the sensitivity matrix contains the output sensitivities for the jth parameter, computed from central finite differences in Eqs. (1–3). The modified Newton–Raphson parameter update is given by[1,6,11]

$$\Delta \hat{\theta} \equiv \theta - \hat{\theta}$$

$$= \left[\sum_{i=1}^{N} S(i)^T R^{-1} S(i) \right]^{-1} \sum_{i=1}^{N} S(i)^T R^{-1} [z(i) - \hat{y}(i)] \qquad (9)$$

The parameter vector update from Eq. (9) is added to the current estimate of the parameter vector to approach the true value of the parameter vector. In practice, there are times when the parameter vector update computed from Eq. (9) leads to an increase in the cost function or a divergence. This is because the modified Newton–Raphson step assumes that the current estimate of the parameter vector is near the true value. Using several iterations of a simplex algorithm[12] when the modified Newton–Raphson step produced an increase in the cost was found to be very effective in avoiding divergence and reaching a solution. This approach was followed in the present study.

When repeated application of Eq. (9) converges, an estimate of the measurement noise covariance matrix R can be obtained from the output residuals. The expression for the estimate of R, which maximizes the conditional probability in Eq. (6), is[1-3,6,11]

$$\hat{R} = \frac{1}{N} \sum_{i=1}^{N} [z(i) - y(i)][z(i) - y(i)]^T \qquad (10)$$

The most recent estimated output $\hat{y}(i)$ is substituted for $y(i)$ in Eq. (10) to compute the matrix $\hat{R}$. Often only the diagonal elements of the R matrix are estimated from Eq. (10), enforcing an assumption that the measurement noise sequences for the measured outputs are uncorrelated with one another. This assumption is generally a good one for real flight test data. All estimates of the measurement noise covariance matrix in this work assume a diagonal $\hat{R}$ matrix. Retaining the full $\hat{R}$ matrix could have been done with little conceptual difficulty, but the expected benefits did not warrant the extra computation involved.

The noise covariance matrix estimate $\hat{R}$ was used in the cost function of Eq. (7), and the minimization process described earlier for known R was repeated. Thus, the maximum likelihood estimation proceeds by alternately estimating the noise covariance matrix from Eq. (10), and minimizing the cost function using Eq. (9) with the latest value of the estimated noise covariance matrix. Convergence is reached when the estimated parameter vector $\hat{\theta}$, the estimated noise covariance matrix $\hat{R}$, and the cost $J(\hat{\theta})$ reach nearly constant values.

Since maximum likelihood estimation is asymptotically unbiased,[1-3] the estimated parameter vector $\hat{\theta}$, should be close to the true value θ, and the gradient of the cost function with respect to the parameter vector should be close to zero. From Eq. (7), assuming R is held fixed,

$$\nabla_\theta J(\theta)|_{\theta = \hat{\theta}} \approx - \sum_{i=1}^{N} S(i)^T R^{-1} [z(i) - \hat{y}(i)] \qquad (11)$$

For practical computation, simultaneous satisfaction of the following numerical criteria was used to define convergence of the maximum likelihood estimation:

$$|[\hat{\theta}_j]_k - [\hat{\theta}_j]_{k-1}| < 1.0 \times 10^{-5} \qquad \forall j, \qquad j = 1, 2, \ldots, n_p$$

$$\left| \frac{[\hat{r}_{ii}]_k - [\hat{r}_{ii}]_{k-1}}{[\hat{r}_{ii}]_{k-1}} \right| < 0.05 \qquad \forall i, \qquad i = 1, 2, \ldots, n_o$$

$$(12)$$

$$\left| \frac{J(\hat{\theta}_k) - J(\hat{\theta}_{k-1})}{J(\hat{\theta}_{k-1})} \right| < 0.001$$

$$\left| \frac{\partial J(\theta)}{\partial \theta_j} \right|_{\theta = \hat{\theta}} < 0.05 \qquad \forall j, \qquad j = 1, 2, \ldots, n_p$$

where k denotes the current estimate iteration number and $\hat{r}_{ii}$ denotes the estimate of the ith diagonal element of $\hat{R}$. The approximate expression for the cost gradient with respect to the parameters [Eq. (11)] was used for the last criterion in Eq. (12).

The minimum achievable parameter variances, called the Cramér–Rao lower bounds, are the diagonal elements of the dispersion matrix D (Refs. 1–3 and 6). The dispersion matrix is defined as the inverse of the information matrix M, the latter being a measure of the information contained in the data from an experiment. The expressions for these matrices are[1-3,6]

$$M = \sum_{i=1}^{N} S(i)^T R^{-1} S(i) \qquad (13)$$

$$D = M^{-1} = \left[\sum_{i=1}^{N} S(i)^T R^{-1} S(i) \right]^{-1} \qquad (14)$$

The square root of the jth diagonal element of D gives the Cramér–Rao lower bound for the standard error of the jth parameter estimate,

$$\sigma_j = \sqrt{d_{jj}} \qquad j = 1, 2, \ldots, n_p \qquad (15)$$

It can be seen from Eqs. (9) and (14) that the dispersion matrix is computed when determining the modified Newton–Raphson step as part of the conventional maximum likelihood estimation. The assumption that the output residuals are white and, therefore, uncorrelated in time is implicit in the algorithm and indicated in Eq. (5). The next section details the theory involved in accounting for arbitrary colored output residuals, which are correlated in time.

When the maximum likelihood estimation has converged, the estimated parameter vector will be close to the true value and Eq. (9) holds. Define the residual vector

$$v(i) \equiv z(i) - \hat{y}(i) \qquad i = 1, 2, \ldots, N \qquad (16)$$

The estimated parameter covariance matrix can be expressed using Eq. (9) with substitutions from the definitions in Eqs. (14) and (16),

$$cov(\hat{\theta}) \equiv E\{(\hat{\theta} - \theta)(\hat{\theta} - \theta)^T\}$$

$$= E\left\{ \sum_{i=1}^{N} \sum_{j=1}^{N} D S(i)^T R^{-1} v(i) v(j)^T R^{-1} S(j) D \right\} \qquad (17)$$

If it is assumed that the discrete noise covariance matrix and the output sensitivities do not depend on the parameter vector estimate at the maximum likelihood solution, then the estimated parameter covariance matrix can be written as

$$cov(\hat{\theta}) = D \left[\sum_{i=1}^{N} \sum_{j=1}^{N} S(i)^T R^{-1} E\{v(i)v(j)^T\} R^{-1} S(j) \right] D \qquad (18)$$

When the output residuals are assumed to be zero mean white [cf. Eq. (5)], then

$$E\{v(i)v(j)^T\} = R\delta_{ij} \qquad (19)$$

From Eqs. (14), (18), and (19), it is easy to see that the parameter covariance matrix reduces to the dispersion matrix D when the output residuals are white.

By definition, when v is a zero mean weakly stationary random process,[13]

$$E\{v(i)v(j)^T\} = \Re_{vv}(i-j) = \Re_{vv}(j-i) \qquad (20)$$

where $\Re_{vv}(i-j)$ is the autocorrelation matrix for the output residual vector. The estimated parameter covariance matrix can be computed by substituting for $E\{v(i)v(j)^T\}$ from Eq. (20) into Eq. (18) and using an estimated value for $\Re_{vv}(i-j)$. An estimate for $\Re_{vv}(i-j)$ can be obtained using the colored residuals from conventional maximum likelihood estimation. The autocorrelation estimate accounts for the frequency content of the colored residuals in the expression for the parameter covariance [Eq. (18)]. Substituting Eq. (20) into Eq. (18) results in

$$\text{cov}(\hat{\theta}) = D\left[\sum_{i=1}^{N} S(i)^T R^{-1} \sum_{j=1}^{N} \Re_{vv}(i-j)R^{-1}S(j)\right]D \qquad (21)$$

where $\Re_{vv}(i-j)$ is computed using the discrete unbiased estimate of the output residual autocorrelation[13]:

$$\hat{\Re}_{vv}(k) \equiv \frac{1}{N-k}\sum_{i=1}^{N-k} v(i)v(i+k)^T = \hat{\Re}_{vv}(-k) \qquad (22)$$

Equation (21) is the expression for the parameter covariance matrix for colored residuals, which are correlated in time. Equation (22) was used to estimate $\Re_{vv}(i-j)$ in Eq. (21). The values for D, R^{-1}, and S are from the conventional maximum likelihood estimation. Equations (21) and (22) embody the postprocessing applied to a conventional maximum likelihood solution to account for colored residuals.

Because this technique postprocesses the output residuals from conventional maximum likelihood estimation to correct the Cramér-Rao bounds, all of the properties of conventional maximum likelihood parameter estimation in a practical flight test data analysis application remain unchanged. These properties are discussed in Refs. 2 and 3.

For equation error parameter estimation, the model has a single output

$$z(i) = x(i)^T\theta + \varepsilon(i) \qquad i = 1, 2, \ldots, N \qquad (23)$$

where $x(i)$ is an $n_p \times 1$ vector of regressors at the ith data point and $\varepsilon(i)$ is the equation error. The preceding analysis applies to this case as well, and the equivalents of Eqs. (21) and (22) are

$$\text{cov}(\hat{\theta}) = D\left[\sum_{i=1}^{N} x(i) \sum_{j=1}^{N} \Re_{\varepsilon\varepsilon}(i-j)x(j)^T\right]D \qquad (24)$$

and

$$\hat{\Re}_{\varepsilon\varepsilon}(k) = \frac{1}{N-k}\sum_{i=1}^{N-k} e(i)e(i+k) = \hat{\Re}_{\varepsilon\varepsilon}(-k) \qquad (25)$$

where

$$D = \left[\sum_{i=1}^{N} x(i)x(i)^T\right]^{-1} \qquad (26)$$

and

$$e(i) = z(i) - x(i)^T\hat{\theta} \qquad (27)$$

Results

The longitudinal short period dynamics of the F-18 HARV fighter aircraft at approximately 20-deg angle of attack were studied. The model state equations in wind axes are given by

$$\dot{\alpha} = \frac{\bar{q}S}{mV}\left[C_{Z_\alpha}\alpha + C_{Z_q}\frac{q\bar{c}}{2V} + C_{Z_{\delta_s}}\delta_s + C_{Z_o}^*\right] + q$$

$$+ \frac{g}{V}[\cos(\Phi_m)\cos(\Theta_m)\cos(\alpha) + \sin(\Theta_m)\sin(\alpha)] \qquad (28)$$

$$\dot{q} = (\bar{q}S\bar{c}/I_y)\left[C_{M_\alpha}\alpha + C_{M_q}(q\bar{c}/2V) + C_{M_{\delta_s}}\delta_s + C_{M_o}^*\right]$$

with measurement equations

$$\alpha_m(i) = \alpha(i) + v_1(i)$$

$$q_m(i) = q(i) + v_2(i)$$

$$a_{z_m}(i) = \frac{\bar{q}S}{mg}\left[C_{Z_\alpha}\alpha(i) + C_{Z_q}\frac{q(i)\bar{c}}{2V} + C_{Z_{\delta_s}}\delta_s(i) + a_{z_o}^*\right] + v_3(i)$$

$$i = 1, 2, \ldots, N \qquad (29)$$

assuming that $C_Z \approx -C_L$ and $a_z \approx a_{z_w}$. Initial conditions for the states were computed from the measured time histories of α and q using a time domain smoother.[14] The parameters $C_{Z_o}^*$, $C_{M_o}^*$, and $a_{z_o}^*$ include both aerodynamic and measurement biases.

To validate the new technique for computing Cramér-Rao bounds, 200 Monte Carlo simulation runs were made using various colored measurement noise processes. Each noise sequence had part of its power in the frequencies between 0 and 1 Hz inclusive (roughly the frequency band of the uncorrupted simulation outputs), with the remaining power taken up by white Gaussian noise out to the Nyquist frequency. The narrow-band portion of the colored noise sequence was generated by passing zero mean white Gaussian noise through a fifth-order Chebyshev low-pass filter with frequency cutoff set at 1 Hz. The resulting narrow-band noise was combined with wideband noise from a separate realization of the zero mean white Gaussian noise process. The percentage of the total noise power from the narrow-band noise was determined by a random number with uniform distribution on the interval [0, 100]. The resulting colored noise sequence was then scaled to achieve approximately a 5/1 signal to noise ratio for the simulated noisy output. This procedure was carried out for each individual simulated output on each Monte Carlo run. Figure 1 shows the power spectral density for the colored noise added to α for run 200, where 19% of the noise power was in the frequency range of 0–1 Hz, inclusive. Colored noise sequences generated in this way are representative of residual sequences observed when analyzing real flight test data and were used for that reason.

To make the Monte Carlo simulation runs realistic, the stabilator input was taken from measured data for the F-18 HARV flying a maneuver designed specifically for accurate parameter estimation.[15] The stabilator input is shown as the solid line in Fig. 2. The parameter values used in the simulations (given in column 2 of Table 1)

Table 1 Parameter estimation results for typical Monte Carlo runs

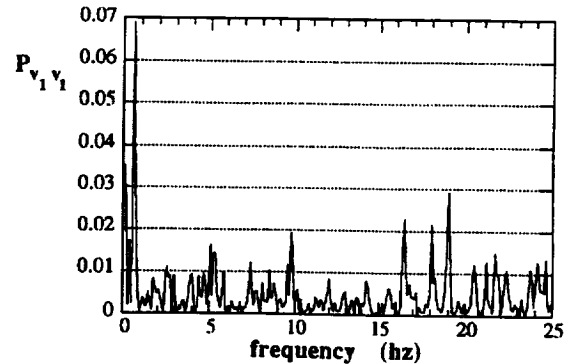|		Run 47			Run 185		
	θ	$\hat{\theta}$	η	η_c	$\hat{\theta}$	η	η_c
C_{Z_α}	−2.00	−1.30	4.24	0.94	−3.78	9.33	2.26
C_{Z_q}	−65.0	−13.8	4.10	0.99	−81.8	1.37	0.33
$C_{Z_{\delta_s}}$	−0.90	−1.48	4.20	0.95	0.04	6.46	1.59
$C_{Z_o}^*$	−0.80	−1.08	4.73	1.04	0.01	10.46	2.33
C_{M_α}	−0.30	−0.35	7.00	1.67	−0.32	3.09	0.48
C_{M_q}	−16.0	−17.3	3.55	0.86	−13.2	7.04	1.13
$C_{M_{\delta_s}}$	−0.70	−0.67	5.42	1.03	−0.72	3.86	0.57
$C_{M_o}^*$	0.08	0.09	5.77	1.20	0.09	5.01	0.73
$a_{z_o}^*$	−0.70	−1.07	6.11	1.36	0.04	9.48	2.14

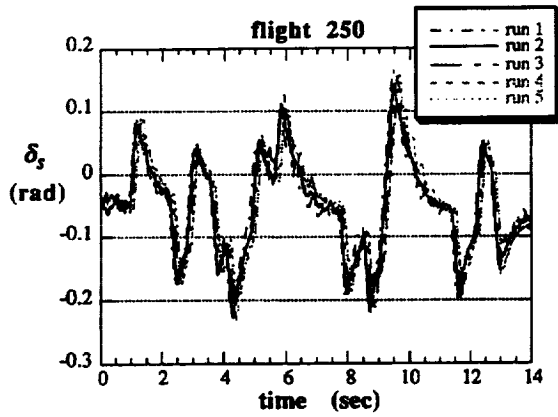Fig. 1 Example simulated colored noise power spectrum, run 200.

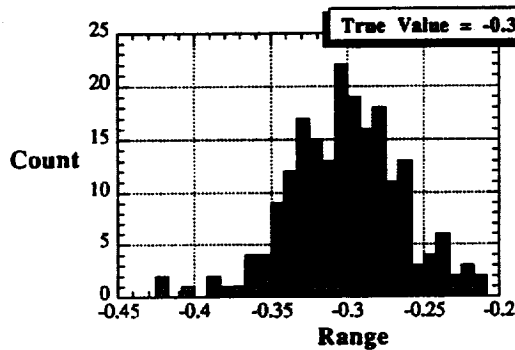Fig. 2 Stabilator input time histories from five repeated flight test maneuvers.

Fig. 3 C_{M_α} estimates from Monte Carlo simulation.

approximately reflect the short period dynamics of the F-18 HARV at 20-deg angle of attack. The stabilator input and parameter values were the same for each simulated data run, so that the information in the data was constant from run to run. The sampling rate was 50 Hz, and the data record length was 14 s. Maximum likelihood estimation as described in the previous section was used to estimate the parameters.

Since the true parameter values were known for the simulated data, the true accuracy of the maximum likelihood estimates could be compared to the accuracy indicated by the Cramér–Rao bound calculations. The conventional Cramér–Rao bounds for the parameter standard errors were denoted by σ and were computed from Eqs. (14) and (15). The Cramér–Rao bounds for the parameter standard errors corrected for colored residuals were denoted by σ_c and were computed as the square root of the diagonal elements of the covariance matrix from Eq. (21), using Eq. (22) to estimate the output residual autocorrelation. Results from both the conventional computation and the corrected calculation were expressed in terms of the ratio of the absolute deviation of each parameter estimate from its true value to the computed Cramér–Rao bound for the parameter standard error. This accuracy measure was assigned the symbol η:

$$\eta \equiv |\hat{\theta} - \theta|/\sigma, \qquad \eta_c \equiv |\hat{\theta} - \theta|/\sigma_c \qquad (30)$$

For a maximum likelihood estimator, the probability distribution of the parameter estimates approaches a Gaussian distribution centered on the true value as the number of data points gets large. Evidence of this can be found in Fig. 3, which is a histogram of the parameter estimates from all 200 Monte Carlo runs for the C_{M_α} parameter. Corresponding histograms for the other estimated parameters were similar. When σ equals the standard deviation of the population of parameter estimates, the quantity $(\hat{\theta} - \theta)/\sigma$ is a standardized normal deviate. It follows that $\eta \le 3$ nearly all of the time when σ is representative of the scatter in the parameter estimates, because a standardized normal deviate lies within ± 3 standard deviations of the mean 99.7% of the time. Analogous statements apply for η_c and σ_c.

Table 1 shows results for two representative Monte Carlo runs. Columns 4 and 5 for run 47 and columns 7 and 8 for run 185 show that the corrected Cramér–Rao bounds accurately reflected the true parameter accuracy, whereas the conventional Cramér–Rao bounds were optimistic (i.e., too small) and produced η ratios that exceeded 3 for almost every estimated parameter. Considering the full set of 200 Monte Carlo runs, Table 2 gives the mean values and standard errors of η and η_c for each estimated parameter. These data show that the conventional Cramér–Rao bounds were inaccurate on the average and exhibited a large variability, whereas the converse was true for the corrected Cramér–Rao bounds.

Table 3 gives another summary of the parameter estimation results for the 200 Monte Carlo simulation runs. The second column of the table gives the mean values of the parameter estimates, and the third column gives the sample standard errors for the parameter estimates, computed from the scatter of the parameter estimates and denoted by s. Columns 4 and 6 give the mean values of the Cramér–Rao bounds for the parameter standard errors computed using the conventional and corrected techniques, $\bar{\sigma}$ and $\bar{\sigma}_c$, respectively. Columns 5 and 7 show the ratio of the sample standard errors for the parameter estimates to $\bar{\sigma}$ and $\bar{\sigma}_c$, respectively. These values are far less than 3 for the corrected calculation of the Cramér–Rao bounds, indicating a proper accounting for the changes in the residual spectra, whereas the conventional calculation of the Cramér–Rao bound was optimistic, producing values of the $s/\bar{\sigma}$ ratio greater than 3.

The data in Tables 1–3 demonstrate that the extent to which the conventional Cramér–Rao bounds misrepresented the true

Table 2 Parameter accuracy statistics for 200 Monte Carlo runs

	Conventional		Corrected	
	$\bar{\eta}$	σ_η	$\bar{\eta}_c$	σ_{η_c}
C_{Z_α}	3.84	2.85	1.37	1.10
C_{Z_q}	3.43	2.72	1.10	0.83
$C_{Z_{\delta_s}}$	3.30	2.51	1.10	0.91
$C_{Z_o}^*$	3.88	2.89	1.36	1.05
C_{M_α}	4.03	3.42	1.44	1.38
C_{M_q}	3.62	2.66	1.26	1.08
$C_{M_{\delta_s}}$	3.63	2.72	1.23	0.88
$C_{M_o}^*$	3.97	3.19	1.37	1.15
$a_{z_o}^*$	3.88	2.80	1.39	1.06

Table 3 Parameter estimation results for 200 Monte Carlo runs

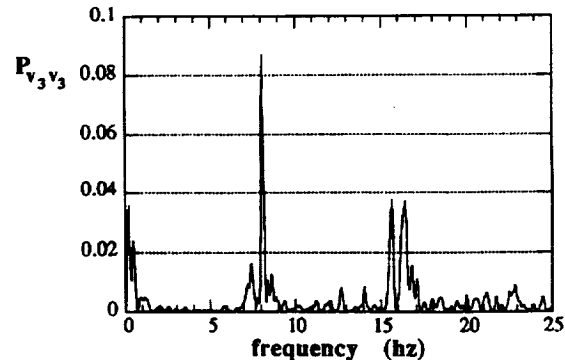|	Simulation		Conventional		Corrected	
	$\bar{\hat{\theta}}$	s	$\bar{\sigma}$	$s/\bar{\sigma}$	$\bar{\sigma}_c$	$s/\bar{\sigma}_c$
C_{Z_α}	−1.94	0.819	0.179	4.56	0.521	1.57
C_{Z_q}	−62.1	51.1	12.3	4.17	38.7	1.32
$C_{Z_{\delta_s}}$	−0.92	0.550	0.139	3.96	0.441	1.25
$C_{Z_o}^*$	−0.82	0.312	0.068	4.56	0.199	1.57
C_{M_α}	−0.30	0.037	0.008	4.80	0.022	1.67
C_{M_q}	−16.1	1.822	0.448	4.07	1.278	1.43
$C_{M_{\delta_s}}$	−0.70	0.030	0.007	4.11	0.021	1.43
$C_{M_o}^*$	0.08	0.013	0.003	4.67	0.008	1.64
$a_{z_o}^*$	−0.72	0.313	0.069	4.54	0.198	1.58

Fig. 4 Power spectrum of a_z residuals, flight test run 1.

parameter accuracy was neither consistent nor predictable from parameter to parameter or from run to run. This phenomenon has been observed previously when analyzing flight test data from repeated maneuvers.[7] It follows that the common practice of applying a fixed correction factor to the conventional calculation of the Cramér–Rao bounds is incorrect to a varying and unpredictable degree in cases where coloring of the residual spectra varies, as in this simulation study. Changes in the coloring of the residuals similar to those studied here can easily be brought about in practice by changes in the model structure, the maneuver, the flight condition, or the instrumentation.

Next, flight test data were analyzed from five repeats of the same longitudinal maneuver, flown on the F-18 HARV at approximately 20-deg angle of attack and 25,000 ft. The input was applied to the
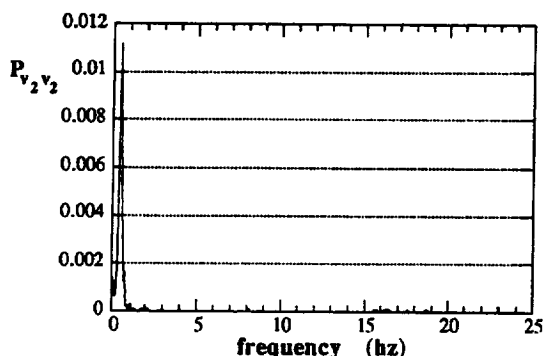

Fig. 5 Power spectrum of q residuals, flight test run 1.

symmetric stabilator by a computerized onboard excitation system (OBES), so that the runs were very nearly repeats of one another. Figure 2 shows the excellent repeatability using the OBES system for five repeated runs of the stabilator input maneuver. All of the data used for analysis were sampled at 50 Hz. Corrections were applied to the angle-of-attack and accelerometer measurements to account for sensor offsets from the center of gravity, and the angle-of-attack measurement was corrected for upwash. Data compatibility analysis[16] revealed that the data from the sensors were consistent to a degree that warranted no further corrections. The same model given in Eqs. (28) and (29) was used for the flight test data analysis, with measured time histories used for V and $\bar{q}$. Maximum likelihood parameter estimation was carried out using the procedure described in the preceding section.

Table 4 gives flight test results in a format similar to Table 3. Column 7 shows that the corrected Cramér–Rao bounds were an accurate measure of the scatter in the parameter estimates. In column 5, the conventional Cramér–Rao bounds were again optimistic for the pitching moment (C_M) parameters but were close to correct for the vertical force (C_Z) parameters. The reason is that the α and a_z measurements are the main influences on the C_Z parameters, and the residuals for both these outputs exhibited considerable power at high frequencies, due to unmodeled structural modes. The power spectrum for a typical a_z residual (from run 1) is shown in Fig. 4. These colored residual spectra roughly resembled constant power out to the Nyquist frequency, which is the assumption made in the theory underlying the conventional Cramér–Rao bound calculation. The q measurement did not have these high-frequency components, and so the conventional Cramér–Rao bound calculation gave very optimistic values for the C_M parameters. The power
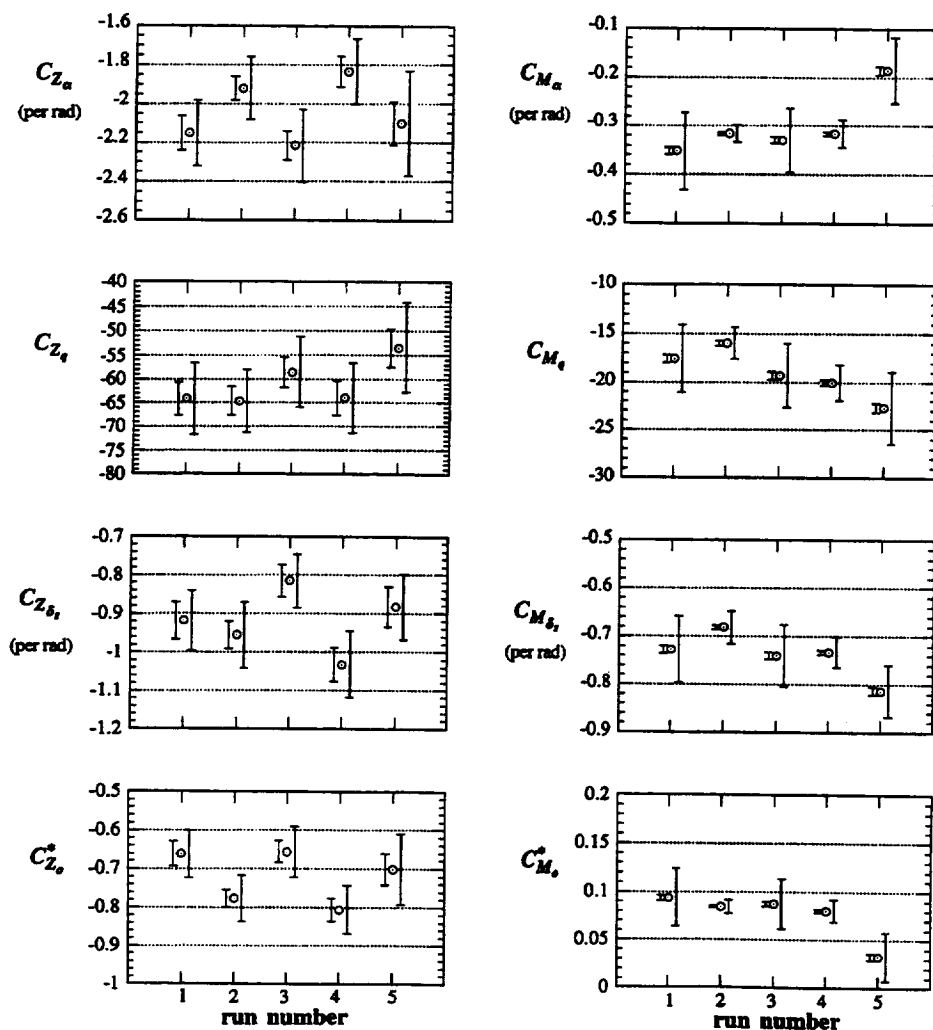

Fig. 6   Parameter estimates with conventional and corrected error bounds: left bar = conventional error bound and right bar = corrected error bound.

Table 4 Parameter estimation results from flight test data

	Flight		Conventional		Corrected	
	$\bar{\theta}$	s	$\bar{\sigma}$	$s/\bar{\sigma}$	$\bar{\sigma}_c$	$s/\bar{\sigma}_c$
C_{Z_α}	−2.04	0.161	0.083	1.95	0.192	0.84
C_{Z_q}	−61.0	4.86	3.48	1.40	7.67	0.63
$C_{Z_{\delta_s}}$	−0.92	0.081	0.044	1.82	0.081	1.00
$C_{Z_o}^*$	−0.72	0.068	0.031	2.21	0.068	1.00
C_{M_α}	−0.30	0.065	0.006	10.80	0.052	1.26
C_{M_q}	−19.1	2.55	0.372	6.86	2.84	0.90
$C_{M_{\delta_s}}$	−0.74	0.048	0.007	6.90	0.051	0.94
$C_{M_o}^*$	0.08	0.025	0.002	10.62	0.020	1.24
$a_{z_o}^*$	−0.66	0.067	0.031	2.17	0.070	0.95

spectrum for a typical q residual (from run 1) is shown in Fig. 5. The corrected calculation of the Cramér–Rao bound worked equally well for the C_Z and C_M parameters because information about the particular coloring of the residuals was incorporated automatically via the autocorrelation estimate from Eq. (22) used in Eq. (21). For the C_{M_α} parameter, the ratio of parameter estimate scatter to the corrected standard error was slightly higher than for the other estimated parameters ($s/\bar{\sigma}_c = 1.26$ from Table 4, column 7). This anomaly was traced to the fact that the control law for the F-18 HARV scheduled leading- and trailing-edge flap deflection in proportion to the angle of attack. The estimated C_{M_α} and C_{Z_α} parameters, therefore, included the effects of the flap deflections, which essentially changed the wing camber. Run 5 began from a slightly different initial trim condition, which caused both leading- and trailing-edge flap deflections to differ from the other runs by 1–2 degrees throughout the maneuver. The change in the effective wing camber was manifested in the C_{M_α} parameter estimate, but not the C_{Z_α} estimate, in agreement with slender wing theory and wind-tunnel data.[17] The true C_{M_α} parameter, therefore, contained variation due to the changes in the effective wing camber, violating the assumption that the parameters should be constant for repeated maneuvers. The result was a larger scatter in the estimates of C_{M_α}, which increased the value of $s/\bar{\sigma}_c$. A similar effect was seen for $C_{M_o}^*$, whose estimated value reflects the trim condition to some extent.

Figure 6 depicts the parameter estimation results for the aerodynamic parameters. The error bars to the left of the round symbols marking the individual parameter estimates represent the Cramér–Rao bounds for the standard errors computed using the conventional calculation ($\pm 1\sigma$). The error bars to the right of the parameter estimate symbols represent the Cramér–Rao bounds for the standard errors from the corrected calculation ($\pm 1\sigma_c$). These plots and the accompanying data in Table 4 show that the standard calculation for the Cramér–Rao bounds gave optimistic values compared to the scatter in the estimates from repeated maneuvers, whereas the corrected calculation for the Cramér–Rao bounds produced Cramér–Rao bounds that accurately reflected the scatter of the estimates.

Concluding Remarks

Algorithms for aircraft parameter estimation using the output error formulation of maximum likelihood are in widespread use. The Cramér–Rao bounds characterizing parameter accuracy that are obtained from conventional calculations are known to be generally optimistic (i.e., too small) in practice, compared to the scatter in parameter estimates from repeated maneuvers. Estimated parameters have limited utility when there is no firm idea of their accuracy. In this work, an expression for correcting Cramér–Rao bounds from maximum likelihood estimation with colored residuals was developed and validated. This result is important because the residuals from maximum likelihood estimation are almost always colored in practice, due to deterministic modeling error. The technique was shown to be applicable to equation error parameter estimation as well.

The calculations involved in the algorithm for computing Cramér–Rao bounds that account for colored residuals can be carried out in a short subroutine called at the conclusion of a conventional maximum likelihood estimation algorithm. Bandwidth of the dominant power in the residuals need not be known or estimated because it is accounted for automatically in the algorithm by an unbiased estimate of the residual autocorrelation. There is no need for correction factors. The algorithm was shown to work for a wide range of colored residual spectra similar to what might be encountered in real flight test data analysis. All calculations are performed in the time domain, obviating the need for frequency domain analysis of the residuals.

The corrected calculation for the Cramér–Rao bounds presented here produced consistently accurate measures of the scatter in the parameter estimates, using an algorithm with moderate computational cost that was applied as a postprocessing of the output residuals from a conventional maximum likelihood solution.

Monte Carlo simulation runs using various colored noise sequences were carried out to validate the algorithm. Analysis of flight data from repeated maneuvers flown on the F-18 HARV demonstrated the validity of the technique for computing appropriate parameter accuracy measures using real flight test data. The algorithm described in this work was shown to be an effective means of accurately determining the quality of parameter estimates from the output error formulation of maximum likelihood estimation.

References

[1]Maine, R. E., and Iliff, K. W., "Identification of Dynamic Systems—Theory and Formulation," NASA RP 1138, Feb. 1985.

[2]Maine, R. E., and Iliff, K. W., "Application of Parameter Estimation to Aircraft Stability and Control—The Output-Error Approach," NASA RP 1168, June 1986.

[3]Maine, R. E., and Iliff, K. W., "The Theory and Practice of Estimating the Accuracy of Dynamic Flight-Determined Coefficients," NASA RP 1077, July 1981.

[4]Murphy, P. C., "A Methodology for Airplane Parameter Estimation and Confidence Interval Determination in Nonlinear Estimation Problems," NASA RP 1153, April 1986.

[5]Murphy, P. C., "Efficient Computation of Confidence Intervals of Parameters," AIAA Paper 87-2624, Aug. 1987; also NASA Tech Brief LAR-14341.

[6]Taylor, L. W., Jr., and Iliff, K. W., "Systems Identification Using a Modified Newton-Raphson Method—A FORTRAN Program," NASA TN D-6734, May 1972.

[7]Klein, V., "Determination of Stability and Control Parameters of a Light Airplane from Flight Data Using Two Estimation Methods," NASA TP-1306, March 1979.

[8]Iliff, K. W., and Maine, R. E., "Further Observations on Maximum Likelihood Estimates of Stability and Control Characteristics Obtained from Flight Data," AIAA Paper 77-1133, Aug. 1977.

[9]Maine, R. E., and Iliff, K. W., "Use of Cramér–Rao Bounds on Flight Data with Colored Residuals," Journal of Guidance and Control, Vol. 4, No. 2, 1981, pp. 207–213.

[10]Balakrishnan, A. V., and Maine, R. E., "Improvements in Aircraft Extraction Programs," NASA CR 145090, 1975.

[11]Morelli, E. A., and Klein, V., "Determining the Accuracy of Maximum Likelihood Parameter Estimates with Colored Residuals," NASA CR 194893, March 1994.

[12]Press, W. H., Flannery, B. P., Teukolsky, S. A., and Vetterling, W. T. Numerical Recipes (FORTRAN version), Cambridge Univ. Press, New York, 1989, Chap. 10.

[13]Bendat, J. S., and Piersol, A. G., Random Data Analysis and Measurement Procedures, 2nd ed., Wiley, New York, 1986, Chaps. 5 and 11.

[14]Graham, R. J., "Determination and Analysis of Numerical Smoothing Weights," NASA TR R-179, Dec. 1963.

[15]Morelli, E. A., "Practical Input Optimization for Aircraft Parameter Estimation Experiments," NASA CR 191462, May 1993.

[16]Klein, V., and Morgan, D. R., "Estimation of Bias Errors in Measured Airplane Responses Using Maximum Likelihood Method," NASA TM 89059, Jan. 1987.

[17]Abbott, I. H., and von Doenhoff, A. E., Theory of Wing Sections, 2nd ed., Dover, New York, 1959, Chap. 7.